Journal of Food Measurement and Characterization
https://doi.org/10.1007/s11694-025-03986-0

ORIGINAL PAPER

# Monitoring of cocoa quality and conching, tempering, cooling processes in chocolate production with FTIR spectroscopy

Yağmur Küçükduman[1,2] · İkra Doğa Korkmaz[1] · Hüseyin Güray Çiftçi[2] · Sinem Argün[1,2] · Gonca Bilge Özel[1] · Özge Taştan Ülkü[1] · Ömer Said Toker[3] · Zeynep Mutlu[4]

Received: 13 October 2025 / Accepted: 18 December 2025
© The Author(s) 2026

**Abstract**
In this study, cocoa quality and process parameters of chocolate production were investigated with ATR-FTIR spectroscopy and chemometrics. Moisture, pH, protein, fat, ash and particle size properties of cocoa samples were correlated with FTIR spectra using the partial least squares (PLS) method to develop a rapid technique. On the other hand, effects of different conching (standard conching, 12 h at 50 °C; 24 h at 50 °C and 12 h at 60 °C; 24 h at 60 °C), tempering (24 °C, 28 °C and 32 °C) and cooling (10 °C and 15 °C) process parameters in chocolate production were monitored with ATR-FTIR. Spectra were evaluated with unsupervised (PCA) and supervised (PLS-DA) chemometric techniques. Results showed that FTIR spectroscopy is a strong tool for rapid quality control of cocoa samples, with $R^2_{pred}$ values above 0.95 and RMSEP values below 0.90 for each quality parameter. The results also showed the potential of FTIR spectroscopy for process control, with 100% prediction sensitivity and specificity in PLS-DA models for conching, tempering, and cooling. The technique demonstrated the ability of FTIR spectroscopy to detect minimal process variations, suggesting its utility in industry for identifying improperly processed chocolates and preventing quality defects.

**Keywords** PLS · PLS-DA · Tempering · Conching · Cooling · Chocolate

## Introduction

Chocolate quality is directly based on raw material quality and process parameters in chocolate production [1, 2]. Therefore, monitoring cocoa bean quality and production processes is essential to ensure the nutritional, economic and sensory attributes of final products. Quality assessment of cocoa products is based on acidity, fat content, protein content, and sensory attributes [3]. However, these quality analysis methods are based on wet chemistry and typically require trained personnel, involve destructive procedures, and are costly. Therefore, quick, real-time, chemical-free and non-destructive methods are needed in the industry.

Production parameters are other quality-affecting factors in chocolates. Chocolate production includes the mixing, refining/conching, tempering, and moulding stages. Among the chocolate production steps, conching is the process of kneading the chocolate at high temperatures (>50 °C) to achieve the appropriate texture and flavour. On the other hand, the tempering process involves melting and cooling the chocolate in a controlled manner to achieve fat crystal form V, the best crystal structure among the six polymorphic forms of cocoa butter [4]. Tempering gives the chocolate its glossy appearance and melt-in-your-mouth properties, while also extending shelf life [5, 6]. Therefore, controlling temperature and the cooling process are also very critical for final product quality. Conventionally, the success of chocolate production steps is generally followed by particle size measurement during conching and by crystal type determination using DSC [7] and X-ray photoelectron spectroscopy [8] for tempering and cooling steps. If improper process parameters

✉ Gonca Bilge Özel
gonca.bilge@yeditepe.edu.tr

1 Department of Food Engineering, Faculty of Engineering and Natural Sciences, Yeditepe University, 34755 Istanbul, Türkiye

2 Department of Biotechnology, Graduate School, Yeditepe University, 34755 Istanbul, Türkiye

3 Department of Food Engineering, Faculty of Chemical and Metallurgical Engineering, Yıldız Technical University, 34210 Istanbul, Türkiye

4 Elvan Gıda San. ve Tic. A.Ş, 34197, Istanbul, Türkiye

Published online: 20 January 2026

are applied, chocolate blooms and surface cracks can occur in the final product. Bloom is one of the primary quality defects in chocolate and is divided into two categories: fat bloom and sugar bloom. Fat bloom is a quality problem that occurs when chocolate is exposed to wide temperature fluctuations, is inadequately tempered, or is held at temperatures above 27 °C. As melted cocoa butter crystals migrate from the center of the chocolate to its surface, they crystallize there, creating a whitish-grey appearance [9]. On the other hand, sugar bloom occurs when storage conditions are inappropriate (relative humidity > 65%) or when the product is rapidly transferred from a low-temperature environment to a high-temperature environment [10]. Both conditions cause the chocolate to sweat and the sugar to melt.

Recently, many spectroscopy-based alternative methods have been developed for rapid analyses of cocoa products. Fourier-transform infrared spectroscopy (FTIR), near infrared spectroscopy (NIR), Fourier-transform near-infrared spectroscopy (FT-NIR), hyperspectral imaging, and Raman spectroscopy [11] are some of them. Spectroscopic techniques are preferred because they are quick, simple, and affordable; they require minimal sample preparation and destruction and no chemicals [12]. In FTIR spectroscopy, compounds such as proteins, lipids, carbohydrates, and water in foods exhibit characteristic absorption bands in the electromagnetic spectrum [13]. Therefore, it can effectively predict multiple quality parameters, such as fat content, moisture content, and flavour compounds, in a single analysis of powdered cocoa samples [14, 15]. In a study, Fourier-transform mid infrared (FT-MIR) spectroscopy, in conjunction with chemometrics, was used to predict the composition of three cocoa samples, including moisture, ash, acidity, fat, and protein content [16].

This study aims to use FTIR spectroscopy to determine the quality parameters of cocoa powder and liquor rapidly, and to investigate the effects of various chocolate production parameters during conching, tempering and cooling using chemometric models. For the first time, this work demonstrates real-time monitoring of chocolate production and shows the ability of FTIR spectroscopy to detect process changes, which shows the potential of FTIR for the determination of process-related quality defects.

## Materials & methods

### Materials

All cocoa samples were received from chocolate and cocoa manufacturers in Türkiye. Sample codes, brand information, and origins of different cocoa groups are presented in Table S1. Additionally, fat and protein values received from suppliers are shown in Table 2. For particle size analyses 2-propanol was supplied from Merck.

### Quality analysis of cocoa powder and liquor samples

All samples were analyzed for moisture content, pH value, ash content and particle size analyses at least two times. Protein and fat results received from suppliers are presented in Table 2.

#### Moisture analysis

The moisture content (%) of cocoa powders was determined using a rapid moisture analyzer (Ohaus, MB45). 5 g of the sample was placed in the sample holder and heated to 103 °C for 5 min. The actual moisture value was then read from the screen. For cocoa liquor samples, the Karl Fischer method was used (ISO 760–1978).

#### pH analysis

pH analyses were performed by mixing 1 g of cocoa powder or cocoa liquor samples with 9 ml of distilled water (80 °C) until entirely dispersed. After the mixture reached room temperature, the pH was measured using a pH meter (MeterLab, PHM210) [17].

#### Ash analysis

The ash content of the samples was determined using the methods described by [18] and [19] with slight modifications. 2 g of cocoa powder samples were placed in a muffle furnace (Nabertherm, B180, Germany) at 550 °C for 6 h. For cocoa liquor samples, the same procedure was performed for 9 h. The ash content was then determined gravimetrically by weighting the samples with crucible after cooling in the desiccator using Eq. 1 [20].

$$\%Ash = \frac{weight\ after\ ashing - tare\ weight\ of\ crucible}{original\ sample\ weight} \times 100 \quad (1)$$

#### Particle size distribution

Particle size analysis of the samples was determined using a laser diffraction particle size analyzer (Malvern Panalytical, Masterizer 3000, UK). Cocoa powders were measured by using the powder feeding unit (Malvern Panalytical, Aero S, United Kingdom) by the dry method without applying any preprocessing of the sample. The measurement parameters are applied as follows: Refractive index, 1.45; absorption index, 0.01; air pressure, 0.4 bar and feed rate, 50%.

Particle size of the cocoa liquor samples was determined using the method described by [21]. The samples were kept at 40 °C for 1–1.5.5 h, and then, a 0.5 g sample was mixed with 10 ml of isopropanol. Samples were measured by the Hydro SV unit of the device. The refractive index was set to 1.59, the absorption index to 0.01, the air pressure to 0.4 bar, and the feeding rate was to 40%. Isopropanol was placed in the sample chamber, and the sample was given to the feeder. The results of the particle size distribution are given as D10, D50 and D90. These values indicate the particle diameter in microns.

## Chocolate production

All chocolate samples were produced using the formulation presented in Table 1. In the production, different process parameters were used as shown in Table 1. For conching processes, five different parameter combinations were used by varying temperature and time. For the tempering process, three different crystallization temperatures, and for cooling, two cooling temperatures were used. The product temperature was regularly monitored using an infrared thermometer (Fluke, 59 MAX) to ensure the process was operating properly.

The mixed formulation was first refined in a chocolate refiner by controlling time and temperature for obtaining fine particles. Then, the melted chocolate was tempered at different tempering temperatures using a chocolate tempering device (Pomati, T5, Italy). The products obtained after the tempering process were poured into heated polycarbonate moulds in a preheated oven (30 ± 1 °C). Then, the moulds were subjected to two different cooling processes using a refrigerated oven (Nucleon, NSI 120) for 30 min. The removed samples were wrapped in aluminum foil and labelled appropriately. The samples were stored at 20 °C.

## FTIR analysis

FTIR spectra of cocoa liquor, cocoa powder and chocolate samples taken from the process were recorded with Nicolet iS10-diamond ATR accessories (Thermo Scientific, USA) and DTGS KBr detector between 4000–500 $cm^{-1}$ wavenumbers. For each measurement, 64 spectra were collected at a resolution of 4 with the aid of Omnic Program (Version 2.8), and each sample was analyzed at least 3 times. Spectra were used for quality analyses and process evaluation in chocolate production. For process monitoring, after conching, tempering and cooling processes, samples were rapidly analyzed with an ATR-FTIR spectrometer.

## Data analysis

Solo 9.3 software (Eigenvector Research Inc., Wenatchee, WA, USA) was used for qualitative and quantitative data analyses.

### Quantitative models

For quantification of quality parameters, the partial least squares (PLS) method was used. In this context, a total of 6 quality parameters (moisture, pH, ash, particle size, protein and fat) were correlated with FTIR spectra to develop a new rapid analysis technique. For all models, the Venetian blinds cross-validation method was used. The best PLS model was obtained with optimum latent variables (LVs) according to the highest correlation coefficient ($R^2$), cross-validated correlation coefficient ($R^2_{cv}$), prediction coefficient ($R^2_{pred}$), lowest root mean square error of calibration (RMSEC), root mean square error of cross validation (RMSECV) and root mean square error of prediction (RMSEP). For this reason, various preprocessing techniques were used, and the models were optimized. All model parameters are presented in Table 3.

### Qualitative models

To investigate similarities/differences among semi-chocolate samples caused by different process parameters in conching, tempering, and cooling, principal component analysis (PCA) as an unsupervised data analysis

**Table 1** Chocolate formulation and process parameters

| Sucrose | Cacao butter | Fat milk powder | Natural Cacao mass | Milk fat (anhydrous) | Emulsifier | Aroma compound | Table salt | Skimmed milk powder |
|---|---|---|---|---|---|---|---|---|
| 53.00% | 24.00% | 10.00% | 10.00% | <1.00% | < 1.00% | < 1.00% | <1.00% | 2.41% |
| **Chocolate production process parameters** | | | | | | | | |
| Proses | | | Conching | | Tempering | Cooling | Storage | |
| Conditions | | | K1: Standard conching* | | T24: 45-24–30 °C | C10: 10 °C, 30 min. | 20 °C | |
| | | | K2: 50 °C–12 h | | T28: 45-28–30 °C | C15: 15 °C, 30 min. | | |
| | | | K3: 50 °C–24 h | | T32: 45-32–30 °C | | | |
| | | | K4: 60 °C–12 h | | | | | |
| | | | K5: 60 °C–24 h | | | | | |

*K1 is the standard conching: 48 °C for 120 minutes, 65 °C for 45 minutes and 55 °C for 120 minutes, respectively

technique and partial least squares-discriminant analysis (PLS-DA) as a supervised data analysis technique were used. For all models, the Venetian blinds cross-validation method was used.

To understand the effects of different process parameters on conching, tempering, and cooling, 3 PCA models were constructed from FTIR spectra collected immediately after each process.

For the supervised classification method, PLS-DA was applied to each process, and 3 models were constructed. To select the best model, the lowest RMSECV and the highest overall sensitivity and specificity were used after trying different preprocessing methods. In PCA and PLS-DA models, 50 raw FTIR spectra for conching, 75 raw FTIR spectra for tempering and 90 spectra for cooling were used.

## Results and discussion

FTIR spectroscopy enables the monitoring of numerous chemical parameters critical to chocolate quality. In finished chocolate products, the technique can accurately predict the sucrose, lactose, fat, and moisture content for quality control purposes [22]. For cocoa, key parameters include moisture content, pH, acidity, fat content, protein levels, and bioactive compounds. In this study, the moisture, pH, particle size, ash, protein, and fat content of cocoa samples were analyzed, and chocolate production steps were monitored using ATR-FTIR spectroscopy. All physicochemical analysis results were presented in Table 2 and used in the PLS models.

### PLS models for quality analyzes

Partial Least Squares (PLS) regression is the most commonly employed chemometric method, enabling the creation of calibration models that relate spectral data to reference analytical values [3, 22]. In this study, physicochemical property predictions of cocoa samples were achieved with the PLS method based on FTIR spectra between 4000–500 $cm^{-1}$ wavenumbers. Within this context, moisture, pH, ash, particle size, fat and protein content prediction models were obtained.

#### Moisture prediction

Moisture content is an important quality parameter in cocoa, as high moisture levels can lead to mould growth and spoilage. In the literature, FTIR spectroscopy has been successfully applied to determine moisture content in cocoa beans, with studies reporting high correlation coefficients (r) of up to 0.96 [15]. In this study, unlike previous studies, prediction models were constructed by using cocoa powder and liquor samples. In Fig. 1a and d, PLS calibration/prediction models and loading plot are presented. For moisture content, approximately 2000–1300 $cm^{-1}$ and 4000 − 3500 $cm^{-1}$ wavenumbers in two regions contributed to the water content (Fig. 1d) [23]. However, -OH bands can also come from alcohol and phenolic substances [24], which can reduce prediction capacity. According to the performance values of the moisture PLS model (Table 3), satisfactory results were obtained with $R^2 = 0.96$ and RMSEP = 0.36.

#### pH analysis

Cocoa can be classified according to the pH values as dark natural (pH 5 to 6), light (pH 6 to 7.2), medium (pH 7.2 to 7.6), or strong alkalized (pH > 7.6) [25]. As in ash content, pH values increase with the degree of alkalization due to the alkaline solutions used to treat cocoa beans [26]. Therefore, the pH values of cocoa samples are good indicators in the industry for the alkalization degree. As an alternative method with FTIR, pH prediction model and loading plot are presented in Fig. 1b and e, respectively. The pH values of the cocoa samples were predicted with $R^2_{pred}$ of 0.96 and RMSEP of 0.22 in the PLS model (Table 3). As shown in Fig. 1e, the loading plot shows that wavenumbers at 3600–3200 $cm^{-1}$, associated with the stretching vibration of the O–H bond, positively affect pH value estimation. Furthermore, there is a positive correlation between the pH values and the inorganic structures observed in the wavenumber range of 1800–600 $cm^{-1}$ [27] in LV1 (Fig. 1e). This indirect relation is caused by alkaline solution treatment for the alkalization process. When alkaline solutions such as NaOH and KOH are added to cocoa, mineral residues remain in its structure. Especially, the presence of peaks around 1400 $cm^{-1}$ may indicate the presence of carbonate groups

**Table 2** The physicochemical analysis results of cocoa powder and liquor samples

| Samples | Moisture (%) | Ash (%) | pH | Particle size (µm) | Protein (%) | Fat (%) |
|---|---|---|---|---|---|---|
| Cacao powder | 2.91 ± 0.02–7.92 ± 0.06 | 5.15 ± 0.01–18.74 ± 0.76 | 5.35 ± 0.04–8.93 ± 0.06 | 13.50 ± 0.52–28.55 ± 0.48 | 21.50 ± 1.09 - 26.50 ± 1.35 | 6.98 ± 0.29–21.00 ± 0.95 |
| Cacao liquor | 0.80 ± 0.05–4.94 ± 0.30 | 2.79 ± 0.13–5.40 ± 0.04 | 4.91 ± 0.01–6.45 ± 0.02 | 5.05 ± 0.33–15.55 ± 1.55 | 11.81 ± 0.57–17.12 ± 0.82 | 48.41 ± 1.84–57.00 ± 2.17 |

*Minimum and maximum values were presented as average

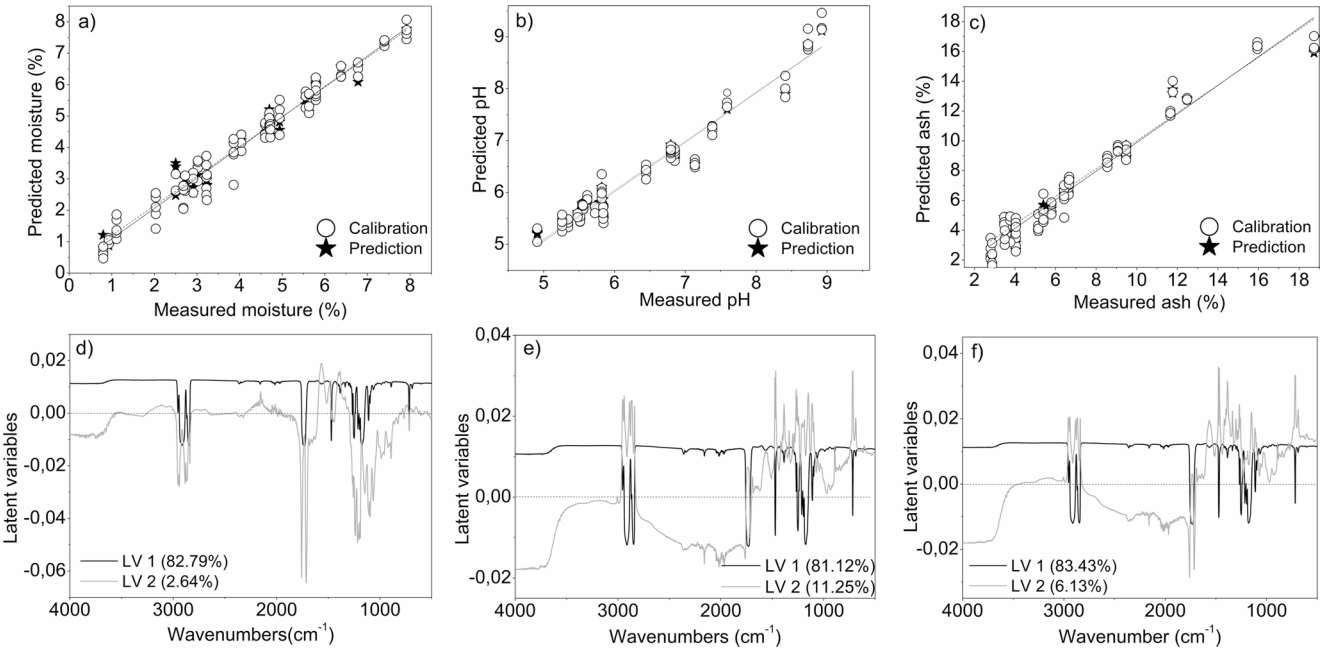



**Fig. 1** PLS models of cocoa samples: moisture calibration/prediction model **a** and loading plot **d**; pH calibration/prediction model **b** and loading plot **e**; ash calibration/prediction model **c** and loading plot **f**

**Table 3** PLS model performance values for quality analyzes of cocoa samples

| Analysis | Number of FTIR spectra | Range of results | Mean of results | Pre-processing | LVs | $R^2_{cal}$ | $R^2_{cv}$ | $R^2_p$ | RMSEC | RMSECV | RMSEP |
|---|---|---|---|---|---|---|---|---|---|---|---|
| Moisture (%) | 134 | 0.76–7.97 | 4.09 | Autoscale | 12 | 0.97 | 0.91 | 0.96 | 0.33 | 0.58 | 0.37 |
| pH | 134 | 4.90–8.97 | 6.34 | Autoscale | 5 | 0.95 | 0.94 | 0.96 | 0.23 | 0.25 | 0.22 |
| Ash (%) | 134 | 2.70–19.27.70.27 | 7.30 | Autoscale | 8 | 0.96 | 0.94 | 0.95 | 0.80 | 0.98 | 0.90 |
| Particle size (µm) | 134 | 4.82–25.10 | 16.04 | Autoscale | 11 | 0.96 | 0.92 | 0.98 | 1.05 | 1.60 | 0.88 |
| Protein (%) | 133 | 11.81–26.50 | 20.20 | Autoscale | 4 | 0.97 | 0.96 | 0.98 | 0.87 | 0.96 | 0.84 |
| Fat (%) | 132 | 6.98–57.00.98.00 | 26.43 | Autoscale | 3 | 0.98 | 0.98 | 0.98 | 2.67 | 2.83 | 2.85 |

[28]. Additionally, the absorption bands of $Na_2CO_3$ and $NaHCO_3$ [29] produced during alkalization are in the range of 1800–702 $cm^{-1}$ wavenumbers [30]. After the alkali treatment (NaOH/KOH addition), carbonate groups increase in the FTIR spectra, indicating a linear correlation between the alkalization degree and pH. Therefore, the peak increment in the fingerprint region contributed to determining the pH value. Araújo et al. [31] also showed the potential of FTIR spectroscopy in pH and acidity determination of coffee samples with 0.78 and 0.92 prediction $R^2$ values.

## Ash analysis

Ash content is an important indicator of total mineral content in foods, including cocoa products. Additionally, there is a strong correlation between ash content and the degree of alkalization in cocoa products. It is known that when the concentration of alkalization solution (NaOH) increases, ash content increases due to the mineral residues left by the alkaline solution. Therefore, high ash content is an undesirable outcome [18] and is important as a quality criterion. In this study, the PLS model for ash content (Fig. 1c) shows high predictive performance, with an $R^2$ of 0.95 and RMSEP of 0.90. All model details are presented in Table 3. According to the loading plot (Fig. 1f), 1800–600 $cm^{-1}$ wavenumbers range positively contributes to the inorganic structure as expected [27], and the loading plot on LV1 approved this relation (Fig. 1f). As mentioned in the pH analysis part, the different absorption bands of the carbonate are found in this wavenumber interval. Inorganic alkaline solutions used during the alkalization process, such as $Na_2CO_3$ and $NaHCO_3$ [29], have characteristic wavenumbers in this range ($Na_2CO_3$: 1775, 1420, 878, and 702 $cm^{-1}$; $NaHCO_3$: 1800 and 1000 $cm^{-1}$) [30]. Sujka et al. similarly achieved that ash measurement in flours by using FTIR spectroscopy [32].

### Particle size analysis

Particle size of cocoa samples affects the textural properties of the final product by changing appearance and mouthfeel [33]. Therefore, particle size is an important quality criterion for cocoa samples. For particle size prediction models, calibration/prediction and loading plot are presented in Fig. 2a and d, respectively. The model's performance metrics indicate high predictive power, with an $R^2_{pred}$ of 0.98 and a RMSEP of 0.88 (Table 3). The loading plot in Fig. 2d shows that the fat peaks (around 1730 and 3000−2750 $cm^{-1}$) are inversely correlated with particle size. This is because the high-fat cocoa liquors used in this study have smaller particles, while the low-fat cocoa powder samples have larger particles (Table 2). This is caused by the cocoa liquor production method. There are some similar studies in the literature on particle size detection with FTIR spectroscopy. In a study conducted by [34], it was found that particle size reduction significantly altered the FTIR spectra of noodles prepared with different sweet potato flours, due to the destruction of carbohydrate and protein structures. In another study [35], showed a correlation between particle sizes of alkali-silica solutions and potassium concentration, as evidenced by bands at 1070–1020 $cm^{-1}$ in the FTIR spectra.

### Protein analysis

Protein is a classical quality criterion for cocoa products. With the aid of strong absorption bands of FTIR spectra mainly in two regions: 1650 $cm^{-1}$ for amide I and around 1550 $cm^{-1}$ (C−N stretching coupled to N−H bending) for amide II [36], protein content was able to be predicted as an alternative rapid method. In this study, protein calibration/prediction model and loading plot for cocoa samples are shown in Fig. 2b and e, respectively. The model provided satisfactory results, with $R^2_{pred}$ of 0.98 and RMSEP of 0.84 (Table 3).

Similarly, a study reported by [16], the developed chemometric models using FT-MIR spectroscopy were used to predict chemical composition of cocoa samples, including moisture, protein, fat, ash, pH, acidity, phenolic compounds, and antioxidant capacity, achieving a SIMCA model reliability of 99% and favorable statistical results for quantitative models ($0.93 < R^2_{cal} < 0.98$). The quantitative models demonstrated strong predictive ability in independent validation, with $R^2_{pred}$ values ranging from 0.93 to 0.97 and standard error of prediction (SEP) values between 0.04 and 3.59, allowing analysis of external cocoa samples.

### Fat analysis

Fat content directly influences the texture and flavour of chocolate, so its amount is significant for chocolate production. As an alternative method, FTIR-based fat prediction models are presented in Fig. 2c and f with $R^2$ values of 0.98 for calibration and 0.98 for prediction, and RMSEP values of 2.85 (Table 3). According to the loading plot, the most relevant wavenumbers with fat content are determined as 1400–1160 $cm^{-1}$ and 3000−2800 $cm^{-1}$,

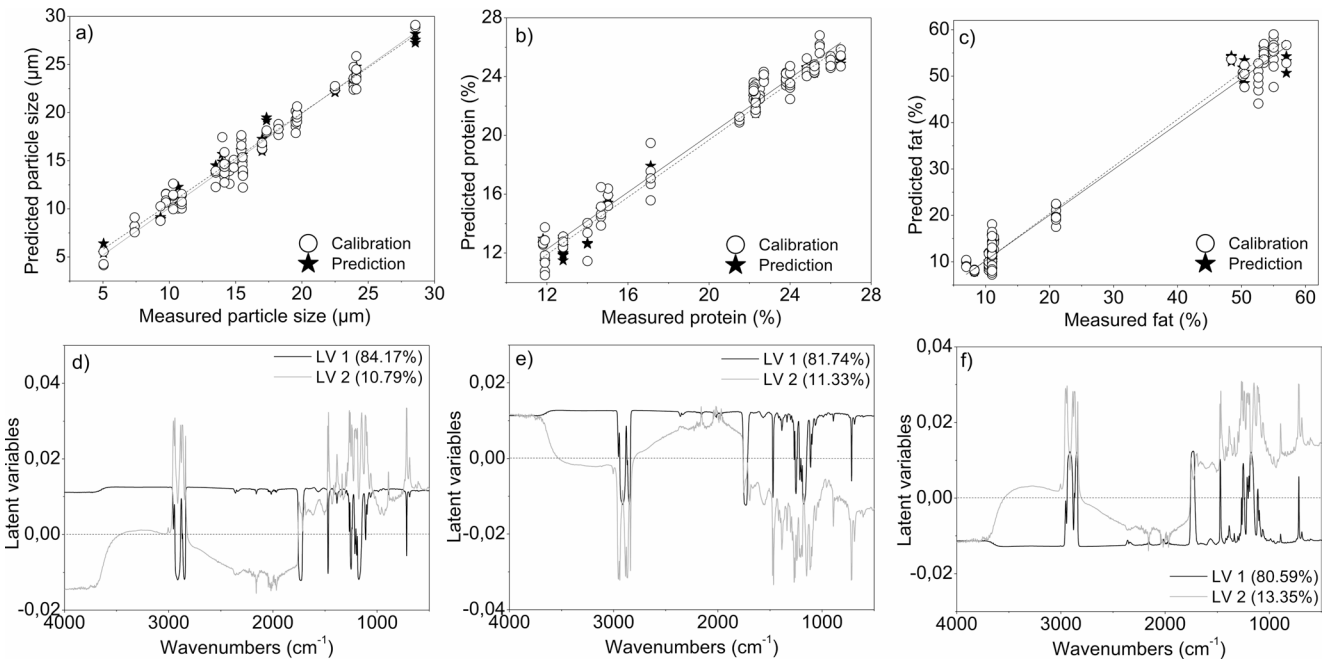



**Fig. 2** PLS models of cocoa samples: particle size calibration/prediction model **a** and loading plot **d**; protein calibration/prediction model **b** and loading plot **e**; fat calibration/prediction model **c** and loading plot **f**

which are related to absorption bands of acyl chains [37, 38] (Fig. 2f). Due to the lack of different fat concentrations having samples in the model, score values are accumulated mainly in two regions in the score plot. Similarly, studies have demonstrated that infrared spectroscopy can predict cocoa fat content, with correlation coefficients (r) ranging from 0.82 to 0.89, depending on the chemometric model used [15, 39].

## Qualitative models: PCA and PLS-DA analyses

Principal Component Analysis (PCA) is frequently used for exploratory data analysis and sample classification [40]. In this study, an unsupervised pattern recognition method was applied to chocolate samples subjected to different conching, tempering, and cooling processes. This way, the effects of different process parameters on the chemical structure can be visualized. For further analyses, the PLS-DA method was used to discriminate chocolate process parameters.

### Conching process

In this study, 5 different conching processes were applied to chocolate mixtures, which were then analyzed by FTIR. In Fig. 3a, differentiating regions of FTIR spectra are presented. To interpret the similarities and differences between samples, the PCA score plot and loading plot are presented in Fig. 3b and c. In the method, only the autoscale preprocess was used as a pretreatment, and 5 principal components (PCs) were selected. In this way, the cumulative variance between samples was 97.70%, with PC1 explaining 64.36% of the variance between samples, and PC2

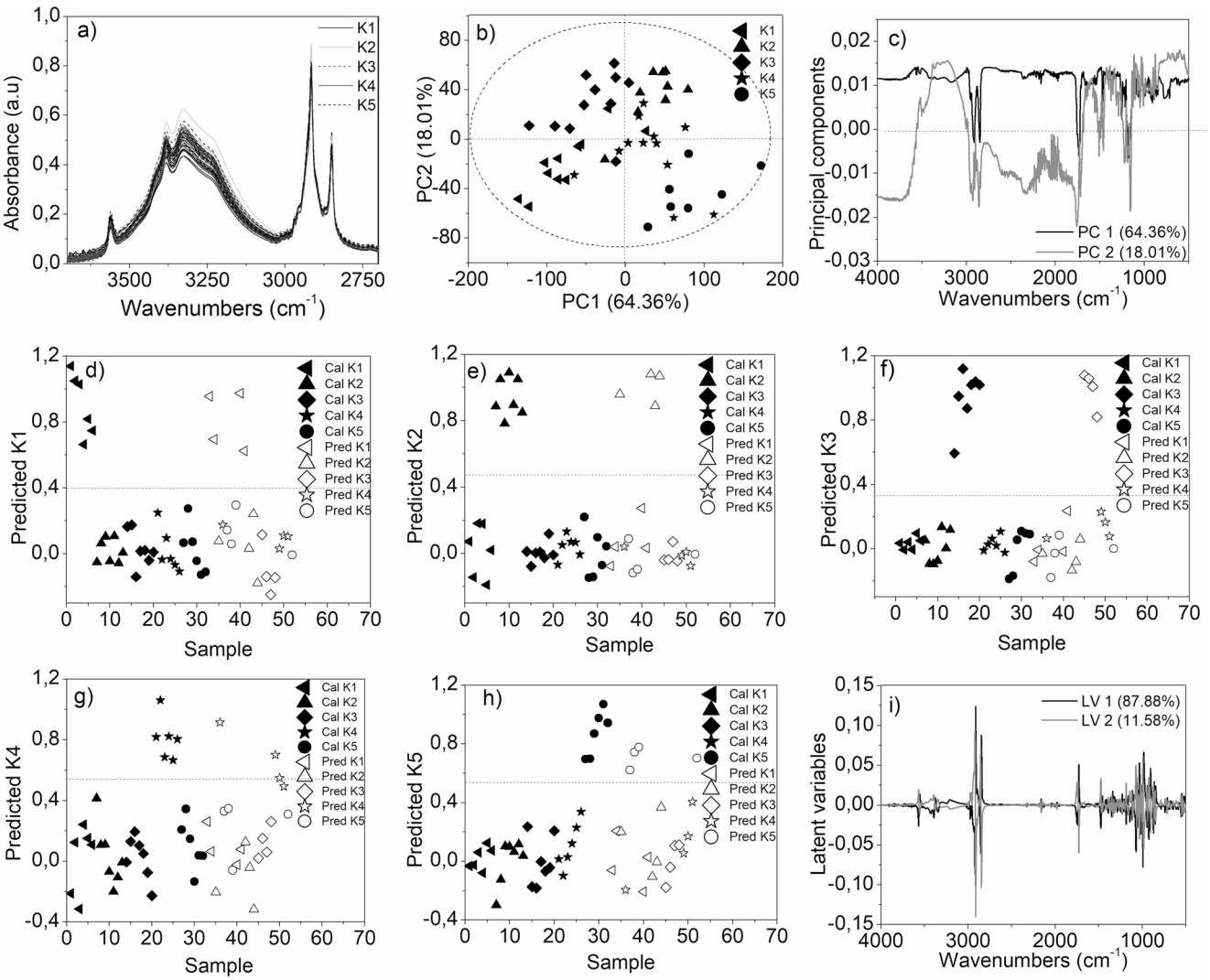



**Fig. 3** FTIR spectra of different conching processes **a**, PCA score plot **b** and PCA loading plot **c**; PLS-DA score plots of different conching processes; K1 discrimination **d**, K2 discrimination **e**, K3 discrimination **f**, K4 discrimination **g**, K5 discrimination **h** and loading plots on LV1 and LV2 **i**

explaining 18.01%. When the score values were examined, it was revealed that samples K4 and K5, i.e., those conched at 60 °C, differed from both the standard conched sample and 50 °C conched sample. When the loading plots that were effective in the separation of these graphs were examined, it was revealed that the peaks at 1157 $cm^{-1}$, 1456 $cm^{-1}$, 1507 $cm^{-1}$, 1742 $cm^{-1}$ and 3000–2500 $cm^{-1}$ showed a negative correlation in PC1 and PC2, while the 3500–3000 $cm^{-1}$ range played a dominant role and showed a positive correlation on PC2 (Fig. 3c).

The conching process causes moisture decrement in chocolate and removal of undesirable volatile residues as the first step [41]. Therefore, as expected, spectral changes occur over time and with temperature. Signal intensity changes around 1745 $cm^{-1}$ were previously observed for roasted coffee beans, corresponding to the vibrations of the (C = O) group of esters [42]. Therefore, signal changes at 1742 $cm^{-1}$ may be assigned to ester group changes during conching. The water content of the samples can be observed in different regions of the FTIR spectra, such as 2100–1300 $cm^{-1}$ and 4000 − 3500 $cm^{-1}$ [23].

Furthermore, the -OH stretching region is observed between 3800–3200 $cm^{-1}$ [43]. Accordingly, it appears that conching affects the wavenumber range of 3500–3000 $cm^{-1}$, where the -OH groups of phenolic compounds are observed. This is because the conching process is directly related to aroma development. Furthermore, since the moisture content of the product is reduced during the conching process, regions where -OH peaks from water molecules are observed were also effective in PCA separation (Fig. 3b).

To further discriminate, the PLS-DA method was applied to samples conched under different conditions (Fig. 3d-h). Model performances are presented in Table 4. Results showed that different conching conditions can be discriminated with 100% calibration and prediction specificity and sensitivity performances. The most relevant peaks for discrimination were between 3000 and 2750 $cm^{-1}$ (Fig. 3i).

## Tempering process

FTIR spectra of samples tempered at 45-24−30 °C (T24), 45-28−30 °C (T28), and 45-32−30 °C (T32) are presented in Fig. 4a to examine the effect of tempering temperature on chocolate structure. Because tempering is related to the crystal structure, the regions at 1800–1700 $cm^{-1}$ and 3000 − 2800 $cm^{-1}$ are included in the spectra.

For unsupervised analysis of the spectra, PCA was performed on FTIR spectra of tempered samples after conching process across all parameters (Fig. 4b and c). The method employed an autoscale preprocess, and the principal component count was set at 4. PCA analysis failed to reveal any differentiation between samples based on different tempers.

**Table 4** PLS-DA performance values of chocolate samples processed under different conching, tempering and cooling parameters

| Calibration results | | | | | Cross validation results | | | | Prediction results | | | |
|---|---|---|---|---|---|---|---|---|---|---|---|---|
| Class: | TPR | FPR | TNR | FNR | TPR | FPR | TNR | FNR | TPR | FPR | TNR | FNR |
| **Conching** | | | | | | | | | | | | |
| K1 | 1.00 | 0.00 | 1.00 | 0.00 | 1.00 | 0.00 | 1.00 | 0.00 | 1.00 | 0.00 | 1.00 | 0.00 |
| K2 | 1.00 | 0.00 | 1.00 | 0.00 | 1.00 | 0.00 | 1.00 | 0.00 | 1.00 | 0.00 | 1.00 | 0.00 |
| K3 | 1.00 | 0.00 | 1.00 | 0.00 | 0.86 | 0.00 | 1.00 | 0.14 | 1.00 | 0.00 | 1.00 | 0.00 |
| K4 | 1.00 | 0.00 | 1.00 | 0.00 | 0.83 | 0.00 | 1.00 | 0.17 | 1.00 | 0.00 | 1.00 | 0.00 |
| K5 | 1.00 | 0.00 | 1.00 | 0.00 | 1.00 | 0.00 | 1.00 | 0.00 | 1.00 | 0.00 | 1.00 | 0.00 |
| **Tempering** | | | | | | | | | | | | |
| T24 | 1.00 | 0.00 | 1.00 | 0.00 | 0.79 | 0.00 | 1.00 | 0.21 | 1.00 | 0.00 | 1.00 | 0.00 |
| T28 | 0.91 | 0.00 | 1.00 | 0.09 | 0.64 | 0.10 | 0.90 | 0.36 | 0.25 | 0.00 | 1.00 | 0.75 |
| T32 | 1.00 | 0.00 | 1.00 | 0.00 | 0.80 | 0.12 | 0.88 | 0.20 | 1.00 | 0.10 | 0.90 | 0.00 |
| **Cooling** | | | | | | | | | | | | |
| C10 | 1.00 | 0.00 | 1.00 | 0.00 | 0.82 | 0.15 | 0.85 | 0.19 | 1.00 | 0.00 | 1.00 | 0.00 |
| C15 | 1.00 | 0.00 | 1.00 | 0.00 | 0.85 | 0.19 | 0.82 | 0.15 | 1.00 | 0.00 | 1.00 | 0.00 |

**TPR* True positive rate, *FPR* False positive rate, *TNR* True negative rate, *FNR* False negative rate

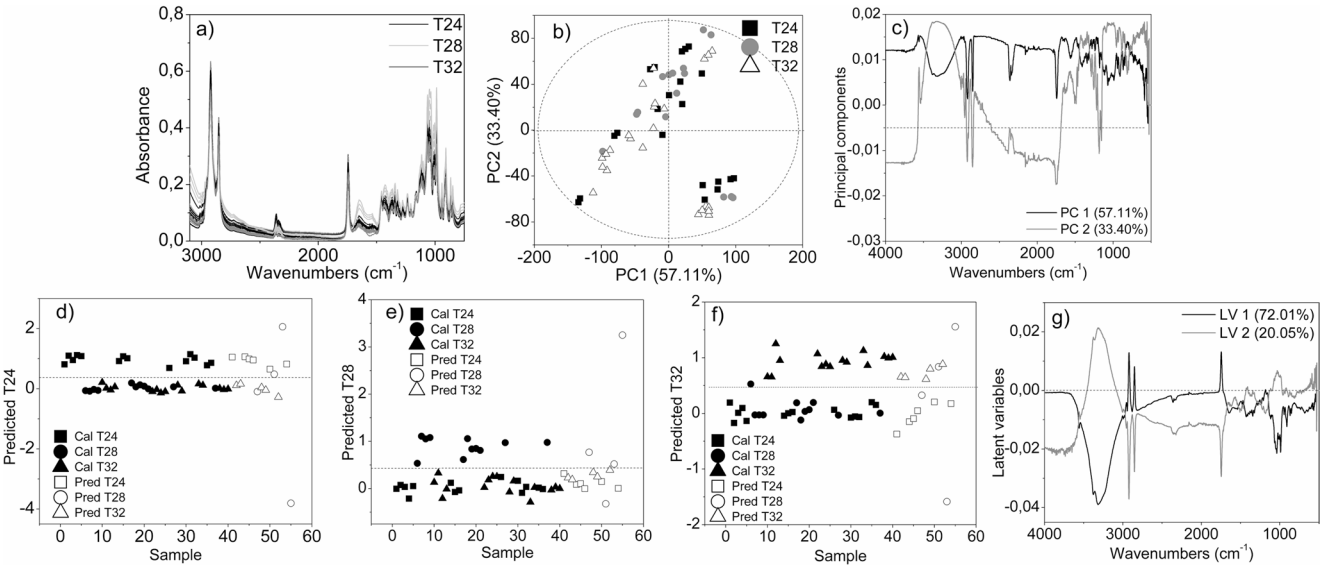



**Fig. 4** FTIR spectra of different tempering processes **a**, PCA score plot **b** and PCA loading plot **c**; PLS-DA score plots of different tempering processes; T24 **d**, T28 **e**, T32 **f** and loading plots on LV1 and LV2 **g**

This is because the samples were separated not only by temper but also within themselves, first by conching parameters and then by tempering parameters. Therefore, no clear distinction was observed using all samples.

FTIR spectra were examined using PLS-DA analysis, a supervised classification technique, for the classification of samples tempered with different parameters (Fig. 4d-f). In the method, the optimum LV number and pretreatment were optimized to achieve the highest sensitivity and selectivity, and the lowest RMSE. Only the mean center was used as the pretreatment, and the number of latent variables (LV) was set to 13. The loading values of the model are shown in Fig. 4g and the performance values are presented in Table 4. Accordingly, it was observed that the directed classification method effectively classified the samples according to their tempering degrees for T24 and T32 samples. However, the prediction capacity of T28 tempering is poor, with a TPR of 0.25. Because the model was confused by the similarities between the T28 and T32 samples. The wavenumbers effective in this classification, as seen in the loading values, were 1722 $cm^{-1}$ and 3000–2800 $cm^{-1}$ in LV1, and 1400–1200 $cm^{-1}$ wavenumbers in LV2 (Fig. 4g). Wavenumbers between 3000–2800 $cm^{-1}$ correspond to 2 important $CH_2$ stretching regions of acyl chains around 2850 and 2920 $cm^{-1}$ [38]. With different molding conditions, these bands changed their shape and frequencies like in the study of [44].

On the other hand, chocolate samples contain various acyl chains, including stearoyl, oleoyl, and palmitoyl groups. When transformed to an ordered structure, each acyl group shows a different series of progression bands between 1400–1160 $cm^{-1}$. The major acyl chains in this system exhibit an intense band around 1180 $cm^{-1}$ in the stable β phase [37], whereas they show a band around 1170 $cm^{-1}$ in the α phase. Therefore, this region includes information about the conformational structure of fats.

Cocoa butter contains the following triacylglycerols (TAGs): 1,3-dipalmitoyl-2-oleoyl glycerol (POP), 1-palmitoyl-2-oleoyl-3 stearoyl glycerol (POSt), and 1,3-distearoyl-2-oleoyl glycerol (StOSt). Symmetrical monounsaturation of these compounds allows the fats to crystallize into six different polymorphisms (I/γ, II/α, III/β2', IV/β1', V/β2, and VI/β1 forms). βV is the most thermodynamically stable form, contributing to chocolate's melting point (ensuring melt-in-the-mouth), gloss, and longevity. The different crystal structures of TAGs cause differences in the intensity and shape of absorption bands. For example, the C=O bands in the glycerol structure of POPs have a wavenumber of 1750–1740 $cm^{-1}$ when the crystal is in a melt or low-stability form, but in high-stability forms, these bands shift to the 1740–1730 $cm^{-1}$ wavenumber range. This is an indication that the glycerol in the structure has restructured and transitioned to a more stable form [45]. Similarly, Kaneko et al. showed that the 1744 $cm^{-1}$ wavenumber can be attributed the glycerol backbone's disordered structure while the 1735 and 1730 $cm^{-1}$ wavenumbers are assigned to its ordered structure [44].

## Cooling process

While the tempering process enables the formation of initial crystal nuclei, the cooling phase promotes crystal growth and the formation of a network structure [2]. The effect of the cooling process at different temperatures (10 °C and 15 °C)

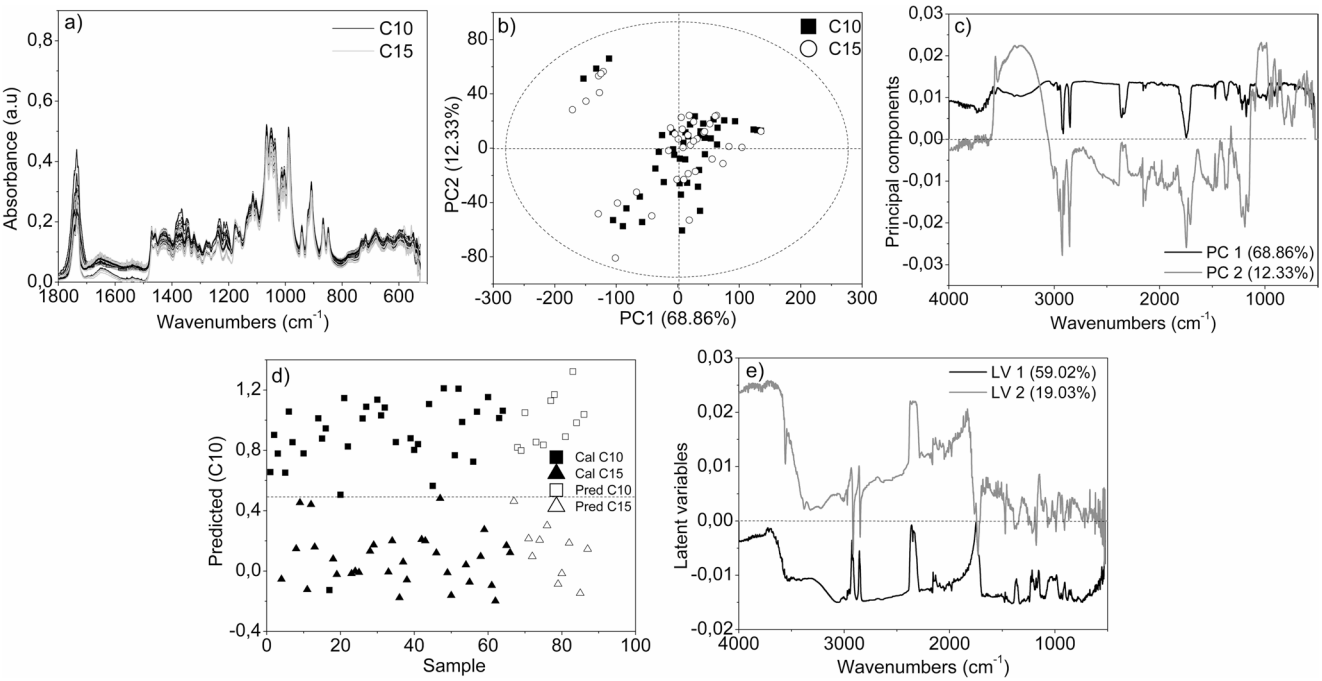



**Fig. 5** FTIR spectra of different cooling processes **a**, PCA score plot **b** and PCA loading plot **c**; PLS-DA score plots of different cooling processes; C10 and C15 **d** and loading plots on LV1 and LV2 **e**

on the FTIR spectra is shown in Fig. 5a, where only significant changes were observed between 1800–500 $cm^{-1}$. Other spectral changes can be monitored in PCA loading plot in Fig. 5c. Accordingly, it was observed that the spectral difference arising from cooling temperatures was minimal. However, it did cause changes in the spectra in the wavenumber ranges 1800–1700 $cm^{-1}$ and 3000−2800 $cm^{-1}$, where fat peaks were generally observed. While a single broad band was observed in the wavenumber range of 1800–1700 $cm^{-1}$ (Fig. 4a) after tempering, three bands began to appear after cooling (Fig. 5a). This is because the chocolate transitions from a liquid, amorphous structure to a more stable, crystalline structure upon cooling [46].

Furthermore, the most important wavenumber range where conformational changes in the acyl chain can be observed is 1180–1160 $cm^{-1}$. Three significant peaks in this region are at wavenumbers 1178, 1170, and 1161 $cm^{-1}$. Accordingly, it is known that more stable beta crystals are formed as the peaks shift to 1180 $cm^{-1}$.

FTIR spectra of samples subjected to different cooling temperatures were analyzed using PCA (Fig. 5b and c). Only autoscale pretreatment was applied to the samples, and the principal component count was selected as 4, which represents the lowest REMSEC and RMSECV (Table 4). The score plot indicates that the samples could not be separated using an undirected principal component analysis (Fig. 5b). This is due to the presence of parameters, such as different conches and tempers, within the sample group. Therefore, more advanced directed classification techniques were needed.

FTIR spectra of samples subjected to 10 °C and 15 °C cooling processes were analyzed using PLS-DA (Fig. 5d), a directed classification method. In the optimal model, autoscale pretreatment was applied to the samples, and 13 latent variables were used. Venetian blinds were used as the cross-validation method (w/6 splits and blind thickness 1). Model performance values are presented in Table 4, and the loading plot is presented in Fig. 5e. An examination of the PLS-DA model performance values reveals that 10 °C and 15 °C cooling processes can be classified. The prediction values indicate that the two cooling degrees can be distinguished with 100% sensitivity, and specificity. This distinction is based on the variability in the polymorphism of oil crystals with different cooling parameters.

## Conclusion

The present study indicates that FTIR spectroscopy is a rapid, chemical-free, and non-destructive alternative for predicting the physicochemical characteristics of cocoa powder and liquor, including moisture, ash, pH, particle size, protein and fat content. On the other hand, FTIR combined chemometrics provided process differentiation within different process parameters in conching, tempering and cooling processes in chocolate production. Results showed that all the chocolate samples are clustered according to the different process parameters in each process. It is based on chemical structure changes within different process parameters.

This study showed the potential use of FTIR spectroscopy to monitor process variables in the food industry that is virtually unexplored in the current literature. These results can contribute to the determination of improper processes in the chocolate industry for an early alert system.

**Supplementary Information** The online version contains supplementary material available at https://doi.org/10.1007/s11694-025-03986-0.

**Acknowledgements** Authors gratefully thank Elvan Gıda for providing cocoa samples.

**Authors' contributions** Conceptualization: Gonca Bilge Özel, Yağmur Küçükduman; Data curation: Yağmur Küçükduman, Gonca Bilge Özel; Methodology: Gonca Bilge Özel, Yağmur Küçükduman, Özge Taştan Ülkü; Formal analysis and investigation: Yağmur Küçükduman; İkra Doğa Korkmaz; Hüseyin Güray Çiftçi, Sinem Argün; Zeynep Mutlu; Writing - original draft preparation: Gonca Bilge Özel, Yağmur Küçükduman; Writing - review and editing: Özge Taştan Ülkü, Sinem Argün; Supervision: Gonca Bilge Özel, Ömer Said Toker; Project administration: Gonca Bilge Özel.

**Funding** Open access funding provided by the Scientific and Technological Research Council of Türkiye (TÜBİTAK). This study was supported by Scientific and Technological Research Council of Turkey (TUBITAK) under the Grant Number 223O050. The authors thank to TUBITAK for their supports.

**Data availability** Data will be made available on request.

## Declarations

**Competing interest** The authors declare no conflict of interest.

**Open Access** This article is licensed under a Creative Commons Attribution 4.0 International License, which permits use, sharing, adaptation, distribution and reproduction in any medium or format, as long as you give appropriate credit to the original author(s) and the source, provide a link to the Creative Commons licence, and indicate if changes were made. The images or other third party material in this article are included in the article's Creative Commons licence, unless indicated otherwise in a credit line to the material. If material is not included in the article's Creative Commons licence and your intended use is not permitted by statutory regulation or exceeds the permitted use, you will need to obtain permission directly from the copyright holder. To view a copy of this licence, visit http://creativecommons.org/licenses/by/4.0/.

## References

1. O.S. Toker, I. Palabiyik, N. Konar, Trends Food Sci. Technol. **91**, 446 (2019)
2. E.J. Windhab, *Beckett's Industrial Chocolate Manufacture and Use* (2017), p.314
3. J.C. Hashimoto, J.C. Lima, R.M.S. Celeghini, A.B. Nogueira, P. Efraim, R.J. Poppi, J.A.L. Pallone, Food Anal. Methods **11**, 1510 (2018)
4. H. Schenk, R. Peschar, Radiat. Phys. Chem. **71**, 829 (2004)
5. T.J. Gutiérrez, Compr. Rev. Food Sci. Food Saf. **16**, 1313 (2017)
6. Ö.S. Toker, H.R. Pirouzian, N. Konar, D.G. Polat, Gıda **43**, 422 (2018)
7. J. Laughter, B. D. Brown, and R. C. Anantheswarn, Specialty Foods: Processing Technology, Quality, and Safety **1**, 157 (2012).
8. B.J. James, B.G. Smith, LWT-Food Science and Technology **42**, 929 (2009)
9. E.O. Afoakwa, A. Paterson, M. Fowler, A. Ryan, Crit. Rev. Food Sci. Nutr. **48**, 840 (2008)
10. E.O. Afoakwa, *Chocolate Science and Technology* (John Wiley & Sons, 2016)
11. M.A. Quelal-Vásconez, M.J. Lerma-García, É. Pérez-Esteve, P. Talens, J.M. Barat, Compr. Rev. Food Sci. Food Saf. **19**, 448 (2020)
12. C.A. Nunes, Food Res. Int. **60**, 255 (2014)
13. Y. B. C. Man, Z. A. Syahariza, M. E. S. Mirghani, S. Jinap, and J. Bakar, Food Chem **90**, 815 (2005).
14. J.J. Permanyer, M.L. Perez, J. Food Sci. **54**, 768 (1989)
15. Z. Zulfahrizal, A.A. Munawar, Trends in Sciences **18**, 31 (2021)
16. L.A. Castillejos-Mijangos, O.G. Meza-Márquez, G. Osorio-Revilla, C. Jiménez-Martínez, T. Gallardo-Velázquez, Foods **12**, 4144 (2023)
17. E. Sioriki, V. Lemarcq, F. Alhakim, H. Triharyogi, E. Tuenter, C. S. J. Cazin, S. P. Nolan, L. Pieters, D. de Walle, and K. Dewettinck, Lwt **145**, 111181 (2021).
18. S. Demirci, C. Elmaci, İ Atalar, O.S. Toker, I. Palabiyik, N. Konar, Food Res. Int. **182**, 114147 (2024)
19. C. Marchioretto, V. Luccas, L.F. Gorup, R.A.B. Gomes, E. Simionatto, K.M.P. de Oliveira, R.P. de Araújo, Â.D.C. Altemio, G.B. Porzani, S.M. Martelli, LWT **191**, 115667 (2024)
20. S. S. Nielsen, *Food Science Text Series Food Analysis*.
21. S. Koca, Bitter Çikolatanın Fizikokimyasal Özellikleri Üzerine Konçlama Şartlarının Etkisi, (2011)
22. J. Tarkošová, J. Čopíková, J. Near Infrared Spectrosc. **8**, 251 (2000)
23. C. Troein, S. Siregar, M. Op De Beeck, C. Peterson, A. Tunlid, P. Persson, Methods Protoc. **3**, 34 (2020)
24. J. O. Ogunkanmi, D. M. Kulla, N. O. Omisanya, M. Sumaila, D. O. Obada, and D. Dodoo-Arhin, Case Studies in Thermal Engineering 12, 711 (2018).
25. K.B. Miller, W.J. Hurst, M.J. Payne, D.A. Stuart, J. Apgar, D.S. Sweigart, B. Ou, J. Agric. Food Chem. **56**, 8527 (2008)
26. E.O. Afoakwa, *Cocoa Production and Processing Technology* (CRC Press, 2014)
27. S. Siregar, A. Nurhikmat, R. Z. Amdani, R. U. Hatmi, M. Kobarsih, A. Kusumaningrum, M. A. Karim, A. H. Dameswari, N. Siswanto, and S. Siswoprayogi, ACS Omega **9**, 32760 (2024).
28. K. Al-Amin, M. Kawsar, M.T.R.B. Mamun, M.S. Hossain, Nanoscale Adv. **7**, 6677 (2025)
29. P.K. Akman, E. Ermiş, C. Daskaya-Dikmen, Ö.S. Toker, J. Food Meas. Charact. **18**, 9410 (2024)
30. N. Đorđević, M. Vlahović, S. Mihajlović, S. Martinović, N. M. Vušović, and J. L. Šajić, Science of Sintering **54**, 481 (2022).
31. C. da S. Araújo, L.L. Macedo, W.C. Vimercati, A. Ferreira, L.C. Prezotti, S.H. Saraiva, J. Sci. Food Agric. **100**, 2488 (2020)
32. K. Sujka, P. Koczoń, A. Ceglińska, M. Reder, H. Ciemniewska-Żytkiewicz, J. Anal. Methods Chem. **2017**, 4315678 (2017)
33. J. Tan, B.M. Balasubramanian, J. Food Eng. **212**, 146 (2017)
34. M. Azeem, S.A. Wadood, T.M. Qureshi, M. Anees. Ur Rehman, I. A. Mohamed. Ahmed, M.O. Aljobair, A.A. Ali, Int. J. Food Prop. **28**, 2433229 (2025)
35. J. Osswald, K.T. Fehr, J. Mater. Sci. **41**, 1335 (2006)
36. A. Barth, Biochimica et Biophysica Acta (BBA)-Bioenergetics **1767**, 1073 (2007)
37. D. Chapman, J. Am. Oil Chem. Soc. **42**, 353 (1965)

38. R. Mendelsohn, R.G. Snyder, Biological Membranes: A Molecular Perspective from Computation and Experiment. (Springer, 1996), pp.145–174
39. A. A. Munawar, Z. Zulfahrizal, and R. Hayati, in (IOP Publishing, 2022), p. 12112.
40. Y. Wang, X. Ma, Y.-D. Wen, Q. Zou, J. Wang, J.-R. Tu, W.-S. Cai, and X.-G. Shao, Spectroscopy and Spectral Analysis **33**, 1226 (2013).
41. N. Konar, Eur. Food Res. Technol. **236**, 135 (2013)
42. M. Rojas S, F. Chejne, H. Ciro, and J. Montoya, J Food Process Eng 43, (2020).
43. E.-P. Ng, S. Mintova, Microchem. J. **98**, 177 (2011)
44. F. Kaneko, K. Oonishi, H. Uehara, H. Hondoh, Cryst. Growth Des. **21**, 3290 (2021)
45. J. Yano, S. Ueno, K. Sato, T. Arishima, N. Sagi, F. Kaneko, M. Kobayashi, J. Phys. Chem. **97**, 12967 (1993)
46. E. Ioannidi, E. Aarøe, S. Balling Engelsen, J. Risbo, F.W.J. den Berg, Food Biophys. **18**, 148 (2023)

**Publisher's Note** Springer Nature remains neutral with regard to jurisdictional claims in published maps and institutional affiliations.